J Solid State Electrochem (2010) 14:1923–1928
DOI 10.1007/s10008-010-1029-5

ORIGINAL PAPER

Scandia-stabilized zirconia-impregnated (La, Sr)MnO_3 cathode for tubular solid oxide fuel cells

Renzhu Liu · Guoqiang Cai · Junliang Li · Chunhua Zhao · Shaorong Wang · Tinglian Wen · Zhaoyin Wen

Received: 14 December 2009 / Revised: 1 February 2010 / Accepted: 5 February 2010 / Published online: 9 March 2010

Abstract We have studied the properties of a LSM-ScSZ composite cathode fabricated by a two-step process including dip-coating LSM framework and ion-impregnating ScSZ, for using with anode-supported tubular solid oxide fuel cells. A preliminary examination of the single tubular cell, consisting of a Ni-YSZ anode support tube, a Ni-ScSZ anode functional layer, a ScSZ electrolyte film, and a LSM-ScSZ cathode fabricated by ion-impregnating, has been carried out, and an improved performance was obtained. The polarization resistance of the cathode side clearly decreased for impregnating the electronic conducting phase (LSM) with the ionic conducting phase (ScSZ). And the single cell with the impregnated cathode generated a maximum power density of 433 mW cm^{-2} at 850 °C, when operating with humidified hydrogen.

Keywords Solid oxide fuel cell · Tubular · Anode-supported · Dip-coating · Composite cathode · Impregnation

Introduction

The solid oxide fuel cell (SOFC) is a completely solid energy conversion device with high efficiency, low noise and low pollution, and convenient fuel flexibility [1–4]. Thus, the use of SOFC technologies can significantly reduce the production of greenhouse gases and pollutants, such as NO_x, SO_x, etc., and improve our environment. As one of the two main designs of SOFCs, tubular structure has many advantages such as the ease of sealing, and their ability to endure the thermal stress caused by rapid heating up to the operating temperature [5–8]. Tubular SOFCs can therefore be expected to be used for co-generation and transportation applications. The resistance of the cathode dominates the total resistance of the anode-supported tubular SOFC [9]. Accordingly, the cathode needs to be optimized first in order for the SOFC to have the potential for commercial application at intermediate temperature.

Sr-doped $LaMnO_3$ (LSM) is the classic cathode material for high-temperature SOFCs because of its good properties, such as electrical conductivity, catalytic activity for oxygen reduction, thermal, and chemical stability at high temperature, and compatibility with electrolytes such as yttria-stabilized zirconia (YSZ) and doped ceria (DCO) [10]. Unfortunately, the oxide ion conductivity of LSM materials is very low and its oxygen trace diffusion coefficient is only approximately 10^{-16} cm^2 s^{-1} at 700 °C [11]. This extremely low oxygen transport ability limits the O_2 reduction reactions to either at or near the triple-phase boundary (TPB) where LSM, electrolyte and O_2 gas meet. However, the electrocatalytic activity of LSM can be improved by mixing it with oxygen ion conducting phases such as YSZ or Gd-doped CeO_2 [12, 13]. Recently, an effective ion-impregnating method [10, 14–19] has been proposed to fabricate a nano-structure composite cathode for planar SOFCs. It is an effective way to impregnate electrocatalytic oxide phase into the porous LSM structure without diminishing the advantages of stability and compatibility of LSM materials with YSZ electrolyte.

In this study, we extend such process to fabricate the LSM-based composite cathode for anode-supported tubular

R. Liu · G. Cai · J. Li · C. Zhao (✉) · S. Wang · T. Wen · Z. Wen
CAS Key Laboratory of Materials for Energy Conversion, Shanghai Inorganic Energy Materials and Power Source Engineering Center, Shanghai Institute of Ceramics, Chinese Academy of Sciences (SICCAS), No.1295 Dingxi Road, Shanghai 200050, People's Republic of China
e-mail: zhaochh@mail.ustc.edu.cn

SOFCs. A porous LSM layer was coated onto a dense $Zr_{0.89}Sc_{0.1}Ce_{0.01}O_{2-x}$ (ScSZ, scandia-stabilized zirconia, Daiichi Kigenso Kagaku Kogyo, Japan) electrolyte using dip-coating and sintering; the ScSZ phase in the cathode was subsequently impregnated into the LSM framework. At the same time, we adopt the impregnation method as a comparison with the previous dip-coating process for preparing LSM-ScSZ composite cathodes on the anode-supported tubular SOFCs.

Experimental

Fabrication of tubular SOFC

The anode-supported thin electrolyte tube, consisting of a NiO-YSZ anode support tube, a NiO-ScSZ anode functional layer, and a ScSZ electrolyte film, was prepared using dip-coating and co-sintering techniques [9]. The length of the tube was approximately 11.0 cm and the outside diameter of the tube was approximately 1.0 cm.

To prepare the cathode, $La_{0.8}Sr_{0.2}MnO_{3-\delta}$ (LSM, 5.78 m^2 g^{-1}, fuelcellmaterials.com) was mixed with graphite (20 wt.%), poly-vinyl-butyl (10 wt.%) and an appropriate amount of triethanolamine, polyethylene glycol (PEG 200), and then ball-milled for 3 h to form a uniform LSM slurry. Using the dip-coating method, the LSM cathode precursor was coated to the ScSZ electrolyte and then sintered at 1,200 °C for 2 h in air. The area of the coated LSM was approximately 10.0 cm^2. ScSZ was subsequently introduced into the LSM framework with an ion-impregnating technique. A concentration of 1.0 mol L^{-1} impregnation solution of $Zr_{0.89}Sc_{0.1}Ce_{0.01}(NO_3)_{4-x}$ was prepared from $Zr(NO_3)_4{\cdot}5H_2O$ (99.9%), $Sc(NO_3)_3{\cdot}4H_2O$ (99.9%) and $Ce(NH_4)_2(NO_3)_6$ (99.9%). Ion impregnation was carried out by dipping and placing a drop of the solution on surface of the coating which infiltrated the cathode framework by capillary effect. The sample was then sintered at 800 °C in air for 1 h. At 800 °C, the nitrate salt was decomposed, forming $Zr_{0.89}Sc_{0.1}Ce_{0.01}O_{2-x}$ (ScSZ) oxide phase. The mass of the cathode before and after the impregnation treatment was measured to determine the impregnated oxide loading. The procedure was repeated to increase the ScSZ loading and at the last time the sample was sintered at 1,000 °C in air for 2 h. The ScSZ loading in the impregnated LSM-ScSZ composite cathode was approx. 30 wt.%.

Cell performance test

Tubular SOFC tests were carried out in a single cell test setup [9]. A Pt mesh and Pt lead wires were attached to the surface of the cathode using Pt paste. On the anode side, a Ni foam and Pt lead wire were used as the current collector and were attached using Pt paste. An alumina tube was put inside the tubular single cell and used to lead the fuel gas, and the oxidant was introduced to cathode from the top of the cell. Humidified hydrogen was used as fuel and oxygen as the oxidant. The fuel and oxidant flow rates were controlled at 180 mL min^{-1} and 120 mL min^{-1}, respectively. The current–voltage (*I–V*) curves and electrochemical impedance spectra (EIS) were obtained to evaluate the performance of the cell. The *I–V* curves were obtained by the volt–ampere method. The EIS were obtained using an Electrochemical Workstation IM6ex (Zahner, GmbH, Germany). The impedance spectra of the electrochemical cell were recorded under open circuit, with an amplitude of 20 mV, in the frequency range of 0.03 Hz to 100 kHz. At the same time, the EIS of the anode to reference electrode and the cathode to reference electrode were measured under open circuit. The measurements were carried out at 700–850 °C, in steps of 50 °C. The ohmic resistances (R_{ohm}) were estimated from the high-frequency intercepts with the real axis and the overall polarization resistances (R_P) were directly measured from the differences between the low- and high-frequency intercepts with the real axis.

The long-time stability testing for the tubular SOFC was carried out at a current density of 200 mA cm^{-2} at 800 °C. The electrochemical impedance spectra under open circuit of the cell, the anode side and the cathode side, were recorded after different times.

In order to study the microstructure of the cathode, scanning electron microscope (SEM) images of a cross-section of the cathode were observed with an electron probe microanalyzer (EPMA, JXA-8100, JEOL) before and after the ion impregnation and after the cell operation.

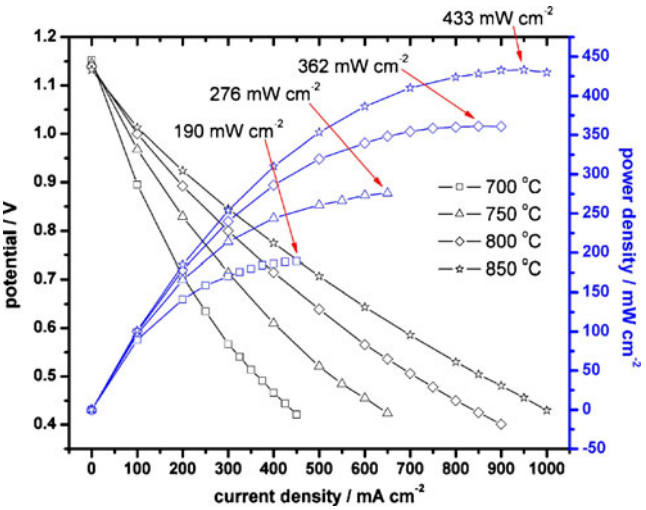

Fig. 1 Typical curves of potential and power density versus the current density for the tubular SOFC with an ion-impregnated cathode while running on humidified hydrogen at different temperatures

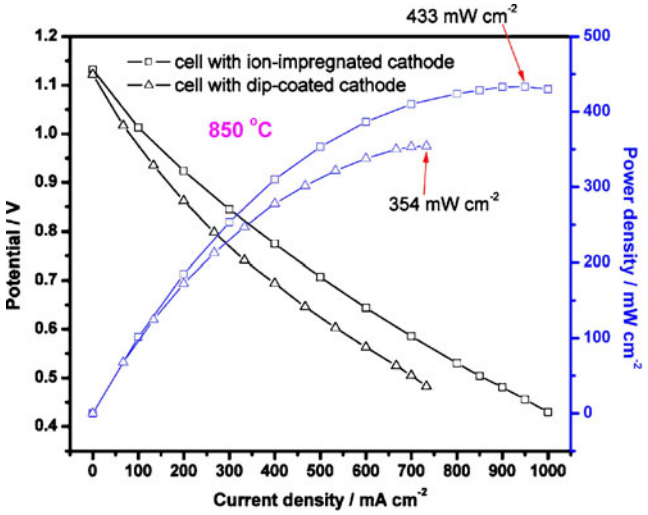

Fig. 2 A comparison of the *I–V* and *I–P* curves for the tubular cells using cathodes fabricated by impregnating and dip-coating methods while operating with humidified hydrogen at 850 °C

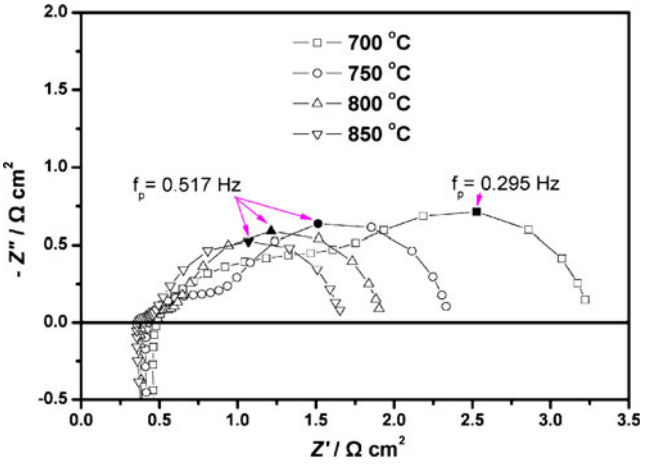

Fig. 3 AC impedance spectra under open circuit for the cell with an impregnated cathode at different temperatures

Results and discussion

Electrochemical performance of anode-supported tubular SOFC

Figure 1 shows typical curves of potential and power density versus the current density for the anode-supported tubular SOFC with an ion-impregnated cathode while running on humidified hydrogen at different temperatures. It can be seen that the anode-supported tubular cell with an effective area of approximately 10 cm^2 produced a good performance, with maximum power densities of 433, 362, 276, and 190 mW cm^{-2} at 850, 800, 750, and 700 °C, respectively. This performance was better than that of the micro-tubular cell with an electrode length of 7 mm of the National Institute of Advanced Industrial Science and Technology (AIST), which produced a power density above 0.13 and 0.30 W/cm^2 at 700 and 800 °C, respectively, in a wet H_2 flow [20]. It was also better than that of the anode-supported flat-tube cell of Advanced Fuel Cell Research Team, Korea Institute of Energy Research, which produced 225 mW cm^{-2} at 750 °C [8]. Also, the performance was clearly improved as compared with that of a previous cell using a dip-coated cathode. A comparison of the *I–V* and *I–P* curves for the tubular cells using cathodes fabricated by the two methods while operating with humidified hydrogen at 850 °C is shown in Fig. 2. A comparison of other performance data for the two cells is given in Table 1.

The AC impedance spectra under open circuit for the cell at different temperatures running on humidified hydrogen are shown in Fig. 3. The R_{ohm} and R_P all increased as the temperature decreased. The R_{ohm} were 0.36, 0.39, 0.43, and 0.49 Ω cm^2 at 850, 800, 750, and 700 °C, while the R_P were 1.29, 1.52, 1.90, and 2.73 Ω cm^2, respectively. Figure 4 shows the AC impedance spectra under open circuit for the single cell, the anode side, and the cathode side at 850 °C. The R_{ohm} and R_P of the single cell, the anode side and the cathode side were, respectively, 0.36 and 1.29 Ω cm^2, 0.10 and 0.37 Ω cm^2, and 0.26 and 0.96 Ω cm^2.

Figure 5 shows the comparison of AC impedance spectra under open circuit for the tubular cells using cathodes fabricated by these two methods while operating with humidified hydrogen at 850 °C. Two depressed arcs were observed in Fig. 5, these results were evaluated by using the equivalent circuit of the Fig. 5. Here, R_{ohm} is ohmic resistance, and (R_1Q_1), (R_2Q_2) represent the high-frequency arc, and low-frequency arc, respectively. Kim et al. [21] suggested that the (R_1Q_1) arc could be interpreted as oxygen ion transfer from the TPB to the electrolyte and it should be related to the length of the TPB. Kim et al. [21] also suggested that the (R_2Q_2) arc represents the diffusion of O^- species along the LSM surface to the TPB and the diffusion of oxygen molecules in electrode pores. So the

Table 1 Maximum power density (MPD), ohmic resistance (R_{ohm}) and the cathode polarization resistance (R_P) at 850 °C of anode-supported tubular SOFCs with different cathodes

	MPD (mW cm^{-2})	R_{ohm} of cell (Ω cm^2)	R_P of cell (Ω cm^2)	R_{ohm} of cathode (Ω cm^2)	R_P of cathode (Ω cm^2)
Dip-coated cathode	354	0.39	1.40	0.28	1.49
Ion-impregnated cathode	433	0.36	1.29	0.26	0.96

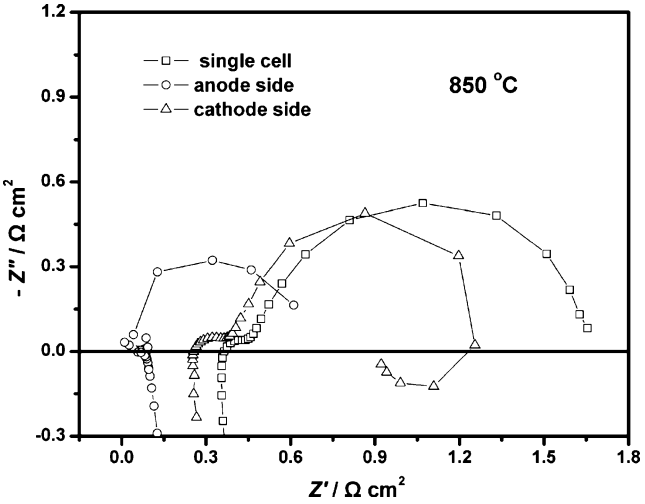

Fig. 4 AC impedance spectra under open circuit for the single cell, the anode side and the cathode side at 850 °C

resistance of the (R_2Q_2) arc is related to not only the length of TPB, but also the porosity of cathode. The oxygen transfer reaction is expressed as:

$$O^{2-} + V_O^{\bullet\bullet} \rightarrow O_O^x \quad (1)$$

Where $V_O^{\bullet\bullet}$ is an oxygen vacancy with two valences, and O_O^x is an oxygen ion in an oxygen ion site. It can be seen that the cell with an ion-impregnated cathode has a much smaller (R_1Q_1) arc compared with that of the cell with a dip-coated cathode. This was due to the ion-impregnating method, which resulted in a nano-sized structure cathode and extended the triple-phase boundary region.

Figure 6 shows AC impedance spectra for the cell with an impregnated cathode under different current densities at 850 °C using humidified H_2 as fuel and O_2 as oxidant. As it

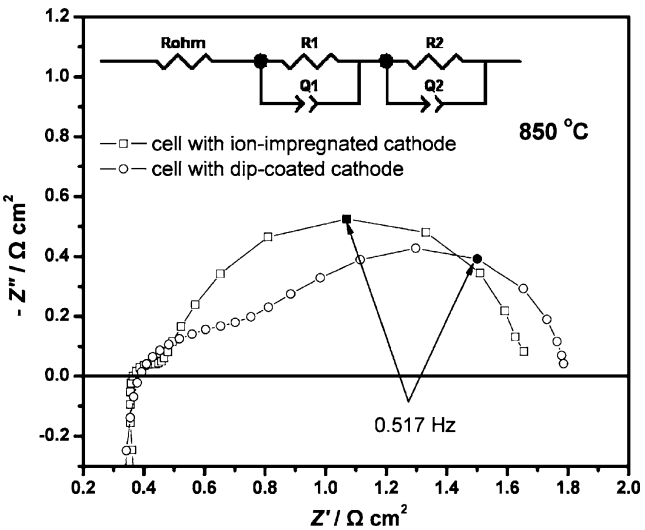

Fig. 5 The comparison of AC impedance spectra under open circuit for the tubular cells using cathodes fabricated by these two methods while operating with humidified hydrogen at 850 °C

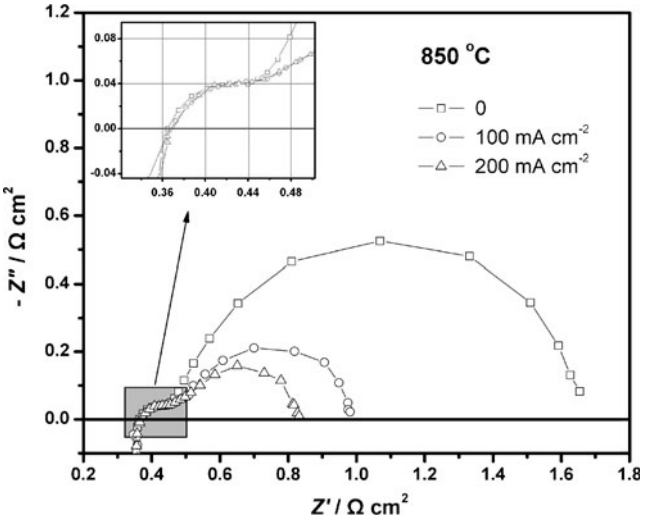

Fig. 6 AC impedance spectra for the cell with an impregnated cathode under different current densities at 850 °C using humidified H_2 as fuel and O_2 as oxidant

can be seen from Fig. 6, the R_{ohm} and (R_1Q_1) arc remained nearly unchanged under different current densities, but the (R_2Q_2) arc decreased clearly as the current density increased. When the LSM electrode is cathodically polarized, Mn^{3+} is reduced to Mn^{2+} and vacancies are created due to charge compensation [22]. This is expressed as:

$$O_O^x(\text{LSM}) + 2Mn_{Mn}^x + V_O^{\bullet\bullet}(\text{electrolyte}) + 2e^- \quad (2)$$
$$\rightarrow V_O^{\bullet\bullet}(\text{LSM}) + 2Mn'_{Mn} + O_O^x(\text{electrolyte})$$

It is thought that oxygen vacancies created on the LSM surface enhance O^- surface diffusion. So the resistance of (R_2Q_2) arc decreased as the current density increased. However, the oxygen vacancies created on LSM surface do not affect oxygen ion transfer, which is a reaction between

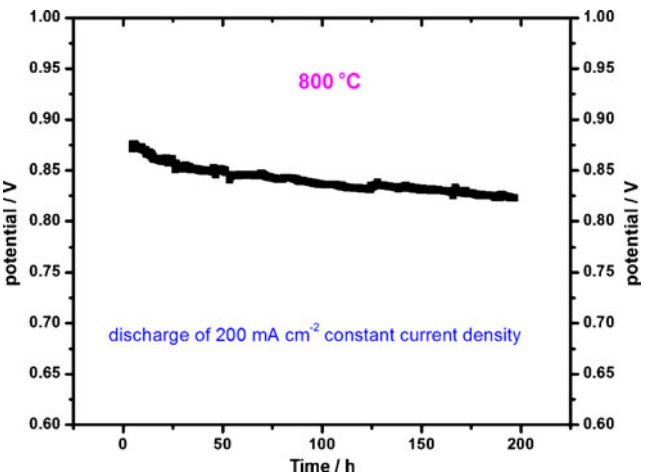

Fig. 7 The voltage change of the cell with an impregnated cathode during a long duration discharge at a current density of 200 mA cm^{-2} at 800 °C

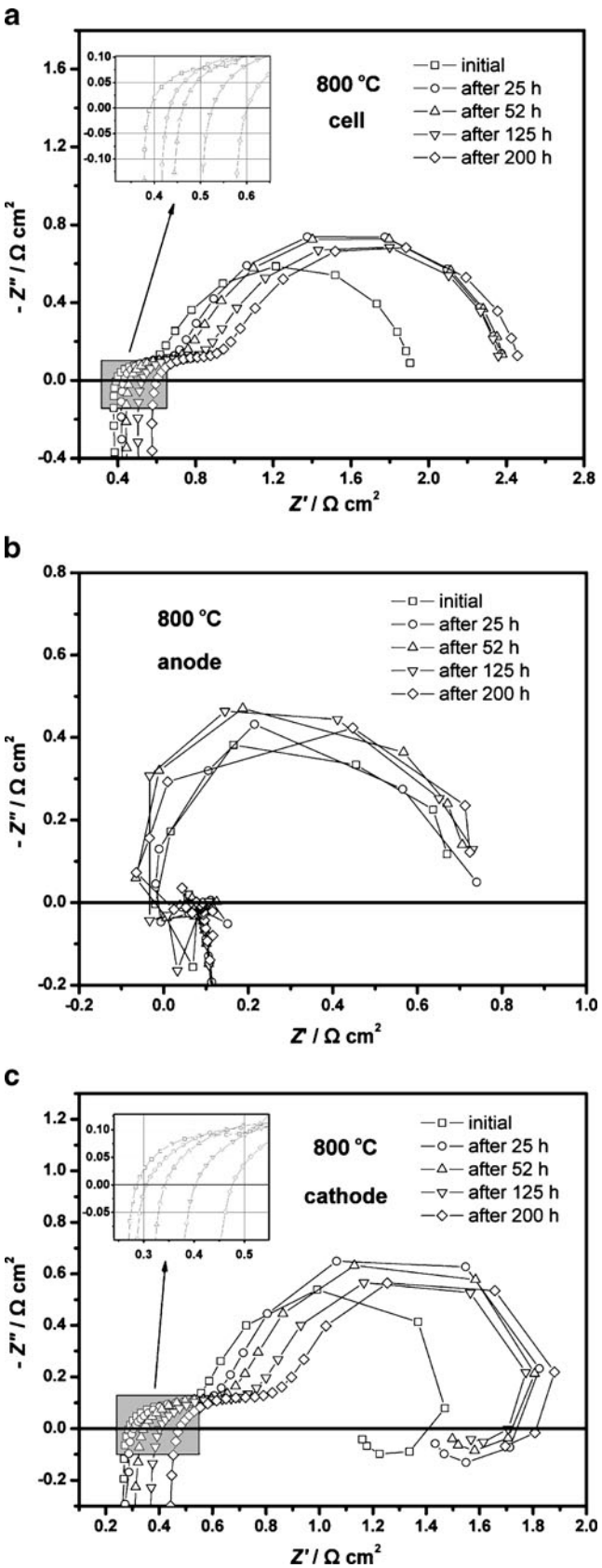

Fig. 8 AC impedance spectra under open circuit for **a** the single cell, **b** the anode side, and **c** the cathode side at 800 °C after different discharge times

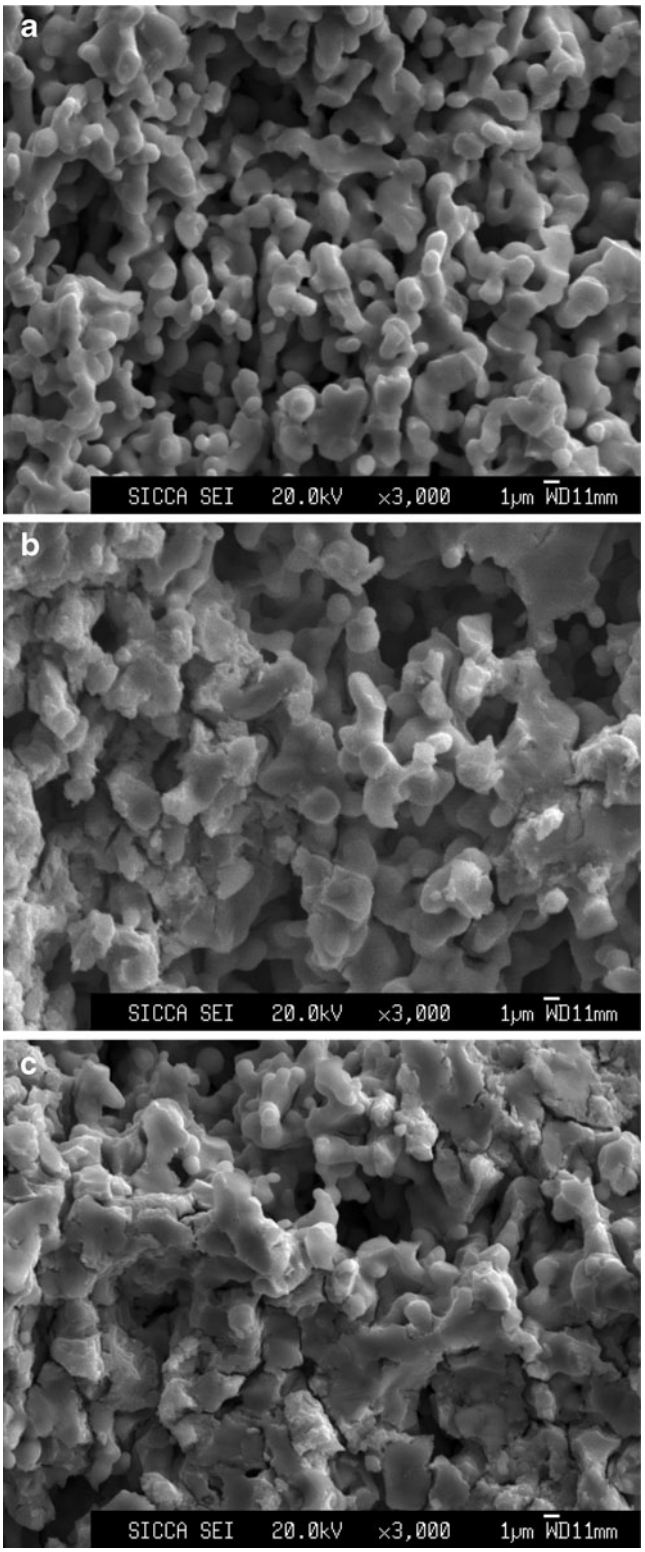

Fig. 9 The SEM micrographs of **a** the LSM framework before ScSZ impregnation, **b** the ScSZ impregnated LSM cathode before cell testing, and **c** the ScSZ impregnated LSM cathode after cell testing

oxygen ions (O^{2-}) at the TPB and oxygen vacancies in the electrolyte.

Long-term stability testing of the tubular SOFC

Figure 7 shows the voltage change of the cell with an impregnated cathode during a long duration discharge at a current density of 200 mA cm^{-2} at 800 °C. It can be seen that the voltage decreased relatively rapidly in the first 25 h, and then slowly in the following 175 h. This may be due to the agglomeration of the ScSZ grains in the cathode in the first time. The reason can be seen by inspection of Fig. 8.

Figure 8 shows the AC impedance spectra for (a) the single cell, (b) the anode side, and (c) the cathode side under open circuit at 800 °C after different discharge times. In Fig. 8, we can see that the R_{ohm} of the cell increased continuously over the test period, and its R_P increased relatively rapidly in the first 25 h, and remains constant later. The change of R_{ohm} and R_P of the cathode in the test time were similar to those of the complete cell. However, the resistance at the anode side did not change. This indicates that the degradation of cell was mainly due to the aging of the cathode, possibly from the agglomeration of the ScSZ grains in the cathode, and the unsealed testing setup, which leads to burning of the unused H_2 and O_2 at the mouth of the tubular cell. The byproduct H_2O and the unburned H_2 may diffuse to the cathode and destroy its structure.

Microstructure characteristics of the cathode

Figure 9 shows the SEM micrograph of (a) the LSM framework before ScSZ impregnated, (b) the ScSZ impregnated LSM cathode before cell testing and, (c) the ScSZ impregnated LSM cathode after cell testing. From Fig. 9a, we found that the LSM framework with an average grain size of approximately 1–2 μm appears as a uniform highly porous structure, which is of great benefit for ion impregnation. After the ScSZ impregnation (Fig. 9b), the nano-sized ScSZ particles were deposited on the LSM grains surface and in the LSM porous structure. The deposition of fine oxygen conducting ScSZ particles on the LSM surface and in the LSM porous structure formed a mutual surrounding structure of ionic conduction phase and electronic conduction phase, which is assumed to effectively extend the TPB region for the O_2 reduction. This structure consequently leads to enhancement of the electrochemical activity and significant reduction of the cathode polarization resistance of the LSM cathodes. But after cell testing (Fig. 9c), the agglomeration of the ScSZ grains in the cathode could be seen obviously. The agglomeration could reduce the TPB region and then increased the cathode polarization resistance.

Conclusions

A LSM-ScSZ composite cathode for anode-supported tubular SOFC has been successfully fabricated by a two-step process including dip-coating LSM framework and ion-impregnating ScSZ. The cell performance was investigated at intermediate temperatures (under 850 °C). The single tubular cell, with area of cathode being approximately 10.0 cm^2, generated 433, 362, 276, and 190 mW cm^{-2} at 850, 800, 750, and 700 °C, respectively, when humidified hydrogen and oxygen were used as the working gases. The AC impedance spectra for the cell indicated that the R_P of the cathode side decreased obviously compared to that of a dip-coated cathode.

Acknowledgments This work is supported by the Postdoctoral Foundation of Shanghai (Grant No. 09R21416600) and the Postdoctoral Foundation of China (No.20080440655, 200902256). The authors thank the CAS Key Laboratory of Materials for Energy Conversion, Shanghai Inorganic Energy Materials and Power Source Engineering Center, Shanghai Institute of Ceramics Chinese Academy of Sciences.

References

1. Mogenson M, Jensen KV, Jørgensen MJ, Primdahl S (2002) Solid State Ionics 150:123
2. Hibino T, Hashimoto A, Inoue T, Tokuno J, Yoshida S, Sano M (2000) Science 288:2031
3. Eguchi K (1997) J Alloys Compd 250:486
4. Du Y, Sammes NM (2004) J Power Sources 136:66
5. Sammes NM, Du Y, Bove R (2005) J Power Sources 145:428
6. Kendall K, Palin M (1998) J Power Sources 71:268
7. Yashiro K, Yamada N, Kawada T, Hong J, Kaimai A, Nigara Y, Mizusaki J (2002) Electrochemistry 70(12):958
8. Kim JH, Song RH, Song KS, Hyun SH, Shin DR, Yokokawa H (2003) J Power Sources 122:138
9. Liu RZ, Wang SR, Huang B, Zhao CH, Li JL, Wang ZR, Wen ZY, Wen TL (2009) J Solid State Electrochem 13:1905
10. Jiang ZY, Zhang L, Feng K, Xia CR (2008) J Power Sources 185:40
11. Souza RAD, Kilner JA, Walker JF (2000) Mater Lett 43:43
12. Murray EP, Barnett SA (2001) Solid State Ionics 143:265
13. Leng YJ, Chan SH, Khor KA, Jiang SP (2004) J Appl Electrochem 34:409
14. Jiang SP, Leng YJ, Chan SH, Khor KA (2003) Electrochem Solid-State Lett 6:A67
15. Jiang SP, Wang W (2005) Solid State Ionics 176:1351
16. Yoon SP, Han J, Nam SW, Lim TH, Oh IH, Hong SA, Yoo YS, Lim HC (2002) J Power Sources 106:160
17. Xu XY, Jiang ZY, Fan X, Xia CR (2006) Solid State Ionics 177:2113
18. Jiang ZY, Zhang L, Cai LL, Xia CR (2009) Electrochimic Acta 54:3059
19. Li JL, Wang SR, Wang ZR, Liu RZ, Ye XF, Sun XF, Wen TL, Wen ZY (2009) J Power Sources 188:453
20. Yamaguchi T, Shimizu S, Suzuki T, Fujishiro Y, Awano M (2008) Mater Lett 62:1518
21. Kim JD, Kim GD, Moon JW, Park YI, Lee WH, Kobayashi K, Nagai M, Kim CE (2001) Solid State Ionics 143:379
22. Jiang Y, Wang S, Zhang Y, Yan J, Li W (1998) J Electrochem Soc 145:373